Nitridomanganese(V) and -(VI) Complexes Containing Macrocyclic Amine Ligands

Karsten Meyer, Jesper Bendix, Nils Metzler-Nolte, Thomas Weyhermüller, and Karl Wieghardt*

Contribution from the Max-Planck-Institut für Strahlenchemie, Stiftstrasse 34-36, D-45470 Mülheim an der Ruhr, Germany

Received March 2, 1998

Abstract: Photolysis of *trans*-[(cyclam)$Mn^{III}(N_3)_2$](ClO_4) (**1**) in methanol at −35 °C with ∼350 nm light produces blue [{*trans*-[(cyclam)$Mn^{V}(N)$]}$_2$(μ-N_3)](ClO_4)$_3$·3H_2O (**2**) and dinitrogen (cyclam = 1,4,8,11-tetraazacyclotetradecane). A series of six-coordinate complexes *trans*-[(cyclam)$Mn^{V}(N)Y]^{n+}$, where Y represents Cl, n = 1 (**3**); CH_3CN, n = 2 (**4**); ClO_4^-, n = 1 (**5**); $CF_3CO_2^-$, n = 1 (**6**), was also synthesized. From a methanol solution of **2** and addition of NaCN the species *cis*-[(cyclam)$Mn^{V}(N)(CN)$](ClO_4) (**7**) was obtained. Photolysis of [$LMn^{III}(N_3)_3$], where L represents the macrocycle 1,4,7-trimethyl-1,4,7-triazacyclononane, in CH_3CN at 20 °C with 253.7 nm light produces colorless crystals of [{$LMn^{II}(N_3)$}$_2$(μ-N_3)$_2$] (**8**) (photoreduction), whereas photolysis with 350 nm light at −35 °C gives the blue photooxidation product [$LMn^{V}(N)(N_3)_2$] (**9**). Complexes **1**−**7** were characterized by X-ray crystallography. Compounds **2**−**7** contain the nitridomanganese(V) unit (Mn≡N 1.51−1.54 **Å**). All nitridomanganese(V) complexes display significant temperature-independent paramagnetism indicative of a low-spin d^2 electron configuration. In the electronic spectra four d−d transitions have been identified for the first time which were unambiguously assigned by single crystal polarized UV/vis/NIR and magnetic circular dichroism (MCD) spectroscopy. The spectra were satisfactorily analyzed in the frame of ligand-field theory (angular overlap method). ^{15}N NMR spectroscopy revealed an enormous deshielding of the nitrido group in **4**, **6**, and **7** (δ = 693−699 ppm referenced to CH_3NO_2 at 0 ppm). Electrochemically, complex **4** undergoes a reversible one-electron oxidation generating a stable nitridomanganese(VI) species (d^1) which has been characterized by UV−Vis and EPR spectroscopy.

Introduction

In 1983 two independent reports on the successful synthesis of the first five-coordinate nitridomanganese(V) complexes containing a terminal Mn≡N group and a porphinato(2−) equatorial ligand appeared in the literature.[1−3] Groves and Takahashi[4] were the first to show that such high-valent nitridomanganese(V) complexes can be used as nitrogen atom transfer reagents to olefins—a theme that has recently attracted considerable interest.[3c,5] Subsequently, the corresponding nitridophthalocyaninatomanganese(V) species were synthesized[6] where the phthalocyaninato(2−) or the phthalocyaninato(1-) π-cation radical constitute the tetradentate equatorial ligands. The first nonporphyrin or nonphthalocyanine ligands were introduced in 1996 by Carreira et al.[7] who prepared [Mn(N)(salen)] and [Mn(N)(saltmen)] complexes (salen = *N*,*N*′-ethylenebis(salicylideneaminato(2−)), saltmen = *N*,*N*′-(1,1,2,2-tetramethylethylene)bis(salicylideneaminato(2−)) in good yields and, more recently, the same group employed Schiff-base type ligands.[8] We reported the first octahedral complex of this type [LMn(N)(acac)]$^+$ (L = 1,4,7-trimethyl-1,4,7-triazacyclononane).[9]

A relatively small number of these nitridomanganese(V) complexes have been structurally characterized by single-crystal X-ray crystallography.[1b,2,7,8,9] In all cases an extremely short Mn≡N bond distance in the range 1.50−1.55 Å has been taken as evidence for a genuine metal−nitrogen triple bond which is in excellent agreement with the observation of the ν(Mn≡N) stretching frequency at ∼1050 cm^{-1} in five-coordinate complexes which decreases to 983 cm^{-1} in the only six-coordinate complex[9] [LMn(N)(acac)]$^+$. A manganese(V) species has a d^2 electron configuration which gives rise to a nonmagnetic, low-spin ground state in Mn^{V}≡N species. Due to the fact that all above complexes display ^1H and ^{13}C NMR signals with "normal" chemical shifts and line widths they have often been characterized as *diamagnetic* species. Careful magnetic susceptibility data reveal that this is an oversimplification as all compounds we have investigated display a substantial temperature-independent paramagnetism, χ_{TIP}, i.e., the molar magnetic susceptibility χ_M corrected for underlying diamagnetism, χ_{DIA}, using Pascal's tabulated constants and taking into account small amounts (<1%) of Curie-paramagnetic impurities, is still *positive*.

(1) (a) Buchler, J. W.; Dreher, C.; Lay, K.-L. *Z. Naturforsch., B: Anorg. Chem., Org. Chem.* **1982**, *37B*, 1155. (b) Buchler, J. W.; Dreher, C.; Lay, K.-L.; Lee, Y. J. A.; Scheidt, W. R. *Inorg. Chem.* **1983**, *22*, 888.

(2) Hill, C. L.; Hollander, F. J. *J. Am. Chem. Soc.* **1982**, *104*, 7318.

(3) Recent Reviews on nitrido complexes: (a) Nugent, W. A.; Mayer, J. M. *Metal−Ligand Multiple Bonds*; John Wiley & Sons: New York, 1988. (b) Dehnicke, K.; Strähle, J. *Angew. Chem.* **1992**, *104*, 978; *Angew. Chem., Int. Ed. Engl.* **1992**, *31*, 955. (c) Du Bois, J.; Tomooka, C. S.; Hong, J.; Carreira, E. M. *Acc. Chem. Res.* **1997**, *30*, 364.

(4) Groves, J. T.; Takahashi, T. *J. Am. Chem. Soc.* **1983**, *105*, 2073.

(5) Bottomley, L. A.; Neely, F. L. *J. Am. Chem. Soc.* **1988**, *110*, 6748.

(6) (a) Grunewald, H.; Homborg, H. *Z. Naturforsch., B: Anorg. Chem., Org. Chem.* **1990**, *45b*, 483. (b) Grunewald, H.; Homborg, H. *Z. Anorg. Allg. Chem.* **1992**, *608*, 81.

(7) Du Bois, J.; Hong, J.; Carreira, E. M.; Day, M. W. *J. Am. Chem. Soc.* **1996**, *118*, 915.

(8) Du Bois, J.; Tomooka, C. S.; Hong, J.; Carreira, E. M.; Day, M. W. *Angew. Chem.* **1997**, *109*, 1722; *Angew. Chem., Int. Ed. Engl.* **1997**, *36*, 1645.

(9) Niemann, A.; Bossek, U.; Haselhorst, G.; Wieghardt, K.; Nuber, B. *Inorg. Chem.* **1996**, *35*, 906.

S0002-7863(98)00686-6 CCC: $15.00 © 1998 American Chemical Society
Published on Web 07/11/1998

Scheme 1. Complexes and Labels

trans-[(cyclam)$Mn^{III}(N_3)_2$](ClO_4) **1**

[{*trans*-[(cyclam)$Mn^{V}(N)$]}$_2$ (μ-N_3)]$(ClO_4)_3 \cdot 3\,H_2O$ **2**

trans-[(cyclam)$Mn^{V}(N)(Cl)$](ClO_4) **3**

trans-[(cyclam)$Mn^{V}(N)(NCCH_3)$]$(ClO_4)_2$ **4**

trans-[(cyclam)$Mn^{V}(N)(ClO_4)$](ClO_4) **5**

trans-[(cyclam)$Mn^{V}(N)(O_2CCF_3)$](ClO_4) **6**

cis-[(cyclam)$Mn^{V}(N)(CN)$](ClO_4) **7**

[{(L)$Mn^{II}(N_3)$}$_2$ (μ-N_3)$_2$] **8**

[(L)$Mn^{V}(N)(N_3)_2$] **9**

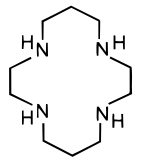

= cyclam

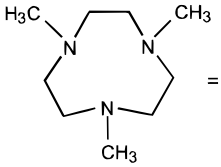

= L

The electronic structure of nitridomanganese(V) species is not well understood. This is mainly due to the fact that the low-intensity d−d transitions have not been identified because the employed equatorial ligands usually display intense charge transfer bands in the UV and even visible region. Only for $[LMn(N)(acac)]^+$ and [Mn(N)(salen)] one or two d−d transitions have been detected,[9,10] respectively, and for the latter species a ligand-field analysis has recently been carried out.[10]

At the outset of the present investigation we decided to prepare a set of nitridomanganese(V) complexes which contain spectroscopically "innocent", i.e., pure σ-donor ligands, which would allow study of the electronic structure of complexes in depth by using a variety of spectroscopic methods. We have discovered that the macrocycle 1,4,8,11-tetraazacyclotetradecane (cyclam) is ideally suited for this purpose and synthesized a series of *trans*-$[Mn^{V}(N)(cyclam)Y]^{n+}$ complexes where the sixth ligand Y represents μ-N_3^-, ClO_4^-, $CF_3CO_2^-$, Cl^-, and CH_3CN (see Scheme 1).

Results and Discussion

Syntheses of Complexes. Nitridomanganese(V) complexes containing tetradentate ligands such as porphinate(2−), phthalocyaninate(2−,1−), salicylidenaminato(salen), or Schiff bases are accessible by either photooxidation of the corresponding azidomanganese(III) species (Arshankow−Poznjak reaction[11]) or by oxidation of suitable manganese(III) precursors in aqueous ammonia solution with NaOCl,[1] iodosylbenzene, or peracetic acid. Recently, Carreira et al.[8] have reported an elegant large scale synthesis using gaseous ammonia and *N*-bromosuccinimide as oxidant. We employ here the above photochemical reaction and the NH_3/NaOCl protocol for the preparation of nitridomanganese(V) complexes of the type $[(cyclam)Mn^{V}(N)(Y)]^{n+}$ where cyclam is the macrocycle 1,4,8,11-tetraazacyclotetradecane and Y is azide, chloride, acetonitrile, perchlorate, trifluoracetate, or cyanide. The new complexes prepared and their labels are summarized in Scheme 1. Schemes S1 and S2 schematically show the synthetic routes to new complexes.

Photolysis of a suspension of *trans*-[(cyclam)$Mn^{III}(N_3)_2$](ClO_4) (**1**)[12] in deaerated CH_3OH at −35 °C with 350 nm light yields after a few hours a clear deep blue solution from which upon addition of solid $NaClO_4 \cdot H_2O$ a microcrystalline blue precipitate of [{*trans*-[(cyclam)$Mn^{V}(N)$]}$_2$(μ-N_3)]$(ClO_4)_3 \cdot 3H_2O$ (**2**) was obtained at −18 °C in ∼50% yield.

On the other hand, treatment at ambient temperature of a suspension of *trans*-[(cyclam)$Mn^{III}(Cl)_2$]$Cl \cdot 5H_2O$ in aqueous ammonia solution (25%) with NaOCl (13% active Cl_2) generates a blue-violet solution and MnO_2. From the filtered solution blue crystals of *trans*-[(cyclam)$Mn^{V}(N)Cl$]PF_6 were obtained upon addition of $NaPF_6$ in moderate yield (18%). The hexafluorophosphate salt was converted to the perchlorate salt (**3**) by metathesis reaction from aqueous HCl by addition of $NaClO_4 \cdot H_2O$.

When an acetonitrile solution of **2** is treated with 1 equiv of $AgClO_4$, a blue-violet solution is obtained after removal of AgN_3 by filtration (Caution: dry AgN_3 is explosive). Addition of dry ethanol to this solution and storage at 4 °C produced blue crystals of *trans*-[(cyclam)$Mn^{V}(N)(NCCH_3)$]$(ClO_4)_2$ (**4**).

Blue-violet crystals of *trans*-[(cyclam)$Mn(N)(OClO_3)$](ClO_4) (**5**) are obtained when the reaction volume of a nitromethane solution of **4** is slowly reduced at 90−95 °C to one-half by evaporation of the solvent. Under these reaction conditions the weakly coordinated acetonitrile ligand in **4** is replaced by a perchlorate ligand in **5**. Complex **4** is a useful starting material for the synthesis of other six-coordinate species *trans*-[(cyclam)$Mn^{V}(N)Y]^{n+}$ because the acetonitrile ligand is very labile. Careful hydrolysis with H_2O of an acetonitrile solution of **4** containing an excess trifluoracetic anhydride yields blue *trans*-[(cyclam)$Mn^{V}(N)(O_2CCF_3)$](ClO_4) (**6**).

In an attempt to generate the corresponding cyano complex *trans*-[(cyclam)$Mn^{V}(N)(CN)$](ClO_4) we treated an acetonitrile solution of **4** (or, alternatively, **2** after treatment with $AgClO_4$) with 2 equiv of NaCN. From the resulting blue solution violet crystals of *cis*-[(cyclam)$Mn^{V}(N)(CN)$](ClO_4) (**7**) were obtained. Under our reaction conditions the *cis*-isomer is thermodynamically more stable than the *trans*-isomer which is in line with the observation that π-acidic ligands (CN^-) prefer to be cis to the Mn≡N group in d^2 complexes.

$$CN^- + \mathbf{4} \rightarrow \{\textit{trans}\text{-}[(\text{cyclam})Mn(N)(CN)]^+\} \rightarrow \textit{cis}\text{-}[(\text{cyclam})Mn(N)(CN)]^+ \quad (1)$$

Photolysis of brown $[LMn^{III}(N_3)_3]$ where L is 1,4,7-trimethyl-1,4,7-triazacyclononane in dry acetonitrile using 185 and 254 nm light in a quartz vessel produces within 60−90 min a colorless solution from which colorless crystals of [{$LMn^{II}(N_3)$}$_2$(μ-N_3)$_2$] (**8**) precipitated in 97% yield. The reaction and the product distribution were found to be independent of the temperature (+20 to −35 °C). This reaction represents a *photoreduction* of the starting complex probably involving homolytic cleavage of an $Mn^{III}-N_3$ bond and generation

$$2\,[LMn^{III}(N_3)_3] \xrightarrow{h\nu} [\{LMn^{II}(N_3)\}_2(\mu\text{-}N_3)_2] + 3N_2 \quad (2)$$

of the $N_3^{\bullet}$ radical which decomposes to dinitrogen, eq 2.

On the other hand, photolysis of the same solution at −35 °C using 350 nm light affords an intensively blue solution. Addition of toluene initiates the precipitation of blue crystals of $[LMn(N)(N_3)_2]$ 0.5 toluene (**9**) in ∼70% isolated yield. *Photooxidation* of $[LMn^{III}(N_3)_3]$ prevails under these conditions, eq 3.

(10) Chang, C. J.; Connick, W. B.; Low, D. W.; Day, M. W.; Gray, H. B. We thank Professor Gray for communicating his results prior to publication.

(11) (a) Arshankow, S. I.; Poznjak, A. L. *Z. Anorg. Allg. Chem.* **1981**, *481*, 201. (b) Arshankow, S. I.; Poznjak, A. L. *Zh. Neorg. Khim.* **1981**, *26*, 1576.

(12) Chan, P.-K.; Poon, C.-K. *J. Chem. Soc., Dalton Trans.* **1976**, 858.

$$[LMn^{III}(N_3)_3] \xrightarrow{h\nu} [LMn^{V}(N)(N_3)_2] + N_2 \quad (3)$$

The above photooxidation is quantitative as was judged by monitoring the change of the UV−vis spectrum of a solution of $[LMn^{III}(N_3)_3]$ upon irradiation (Figure 1). At the beginning of an experiment the spectrum is dominated by very intense ($\epsilon > 4.0 \times 10^3$ L mol^{-1} cm^{-1}) charge-transfer bands $N_3 \rightarrow Mn^{III}$ and $\pi-\pi^*$ transitions of coordinated azide ligands of the starting material $[LMn^{III}(N_3)_3]$ in the range 300−500 nm which are gradually completely bleached. The product spectrum is nearly transparent in this range, but weak d−d transitions at 638 nm ($\epsilon = 100$ L mol^{-1} cm^{-1}) and 1020 nm ($\epsilon \sim 2$ L mol^{-1} cm^{-1}) appear which are identical to the spectrum of a genuine sample of **9** in CH_3CN. The $\pi-\pi^*$ transition of coordinated azide is shifted to 280 nm ($\epsilon = 6.8 \times 10^3$ L mol^{-1} cm^{-1}).

Visible light with $\lambda_{max} = 420$ nm does not induce photoreduction or photooxidation of $[LMn^{III}(N_3)_3]$—no spectral changes were observed within 5 h at −35 °C or ambient temperature. Irradiation of **1** in CH_3CN with ultraviolet radiation (185 and 254 nm) leads to complete destruction of the complex. No isolable products were obtained. It is conceivable that the $N_3^\bullet$ radicals attack the secondary amine groups of the ligand cyclam.

Similar experiments have been performed on $[(ttp)Mn^{III}(N_3)]$ where ttp represents tetraphenylporphinate(2−) in 2-methyltetrahydrofuran using γ-rays (^{60}Co-γ-ray) or visible light (440−750 nm) in which the photoreduced $[(ttp)Mn^{II}]$ and -oxidized $[(ttp)Mn^{V}(N)]$ forms have been described.[14] The $N_3^\bullet$ radical has in the case of photoreduction been detected by using the spin trap phenyl-*N*-*tert*-butylnitron.

We have investigated the electrochemistry of complex **4** in dry acetonitrile containing 0.10 M tetra-*n*-butylammonium hexafluorophosphate as supporting electrolyte at a glassy carbon working electrode. Figure S1 displays the cyclic voltammogram (cv) and a square-wave voltammogram. In the potential range 0.0 to +1.6 V vs the ferrocenium/ferrocene (Fc^+/Fc) couple a single, reversible one-electron-transfer wave is observed at $E_{1/2} = 1.26$ vs Fc^+/Fc. The number of electrons per manganese ion transferred was determined by measuring the peak current function $k = i_p \cdot \nu^{-1/2}$ in the cv and the Cotrell constant $c = i \cdot t^{1/2}$ from a chronoamperometric experiment. The ratio of these two quantities is related to the number of transferred electrons n as in eq 4[15] where i_p is the peak current at a scan rate ν.

$$(i_p \cdot \nu^{-1/2})/i \cdot t^{1/2} = 4.92 \cdot n^{1/2} \quad (4)$$

The number of transferred electrons, n, has been determined to be 1.08 ± 0.05. Since this one-electron process involves oxidation of **4** we assign the process as in eq 5.

$$[(cyclam)Mn^{V}(N)(NCCH_3)]^{2+} \underset{+e}{\overset{-e}{\rightleftharpoons}} [(cyclam)Mn^{VI}(N)(NCCH_3)]^{3+} \quad (5)$$

It therefore appears that the Mn^{VI} oxidation level is accessible. In a coulometric experiment at low temperature (−35 °C) it is possible to generate a yellow solution of this species at +1.30 V vs Fc^+/Fc. The same solution was obtained when a blue acetonitrile solution of **4** was treated with an excess of PbO_2 and a drop of methanesulfonic acid. The UV−vis spectrum of this yellow oxidized species exhibits a broad unsymmetrical absorption maximum at 460 nm ($\epsilon = 100$ M^{-1} cm^{-1}) and resembles closely the spectrum of the isoelectronic $[Cr^{V}(N)(cyclam)(NCCH_3)]^{2+}$ complex.[16]

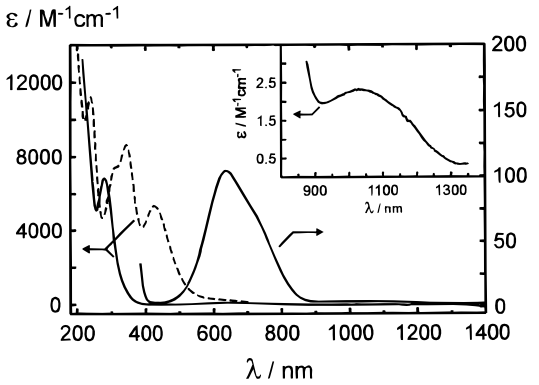

Figure 1. Electronic spectra of $[LMn^{III}(N_3)_3]$ (- - -) and $[LMn^{V}(N)(N_3)_2]$ (—) in CH_3CN.

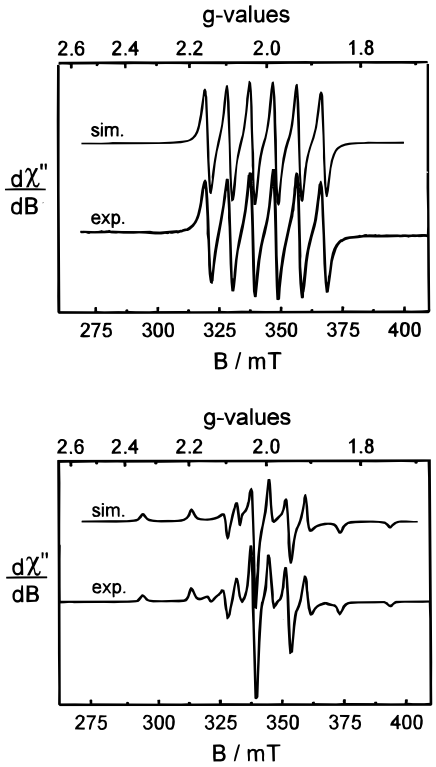

Figure 2. X-band EPR spectra of the electrochemically one-electron oxidized form of **4** in CH_3CN (0.10 M $[N(n\text{-butyl})_4]PF_6$) at 268 K (top) and 10 K (bottom). Experimental conditions: 10 K: frequency 9.6416 GHz, microwave power 0.252 mW, modulation amplitude 11.4 G; 268 K: frequency 9.651 GHz, microwave power 100 mW, modulation amplitude 4.056 G. The simulations at 10 K were performed with Lorentz-shaped lines and m_I-dependent line widths of 1.8 (1+0.015 m_I^2) mT; at 268 K a line width of 1.2 mT was employed.

Figure 2 exhibits the X-band EPR spectra of such a solution measured at 268 and 10 K, respectively. At 268 K an isotropic hyperfine split, (^{55}Mn; $I = {}^5/_2$), six line spectrum at $g \sim 2.0$ is observed. To simulate the increasing distances between the hyperfine signals with increasing magnetic field in the spectrum correctly we employed a full-matrix diagonalization procedure which included not only the usual electronic and nuclear Zeeman hyperfine coupling operator ($S = {}^1/_2$; $I = {}^5/_2$) but also a quadratic

(13) Wieghardt, K.; Bossek, U.; Nuber, B.; Weiss, J. *Inorg. Chim. Acta* **1987**, *126*, 39.

(14) Jin, T.; Suzuki, T.; Imamura, T.; Fujimoto, M. *Inorg. Chem.* **1987**, *26*, 1280.

(15) Ole, H.; Parker, V. D. *Organic Electrochemistry: an Introduction and Guide*, 3rd ed.; Marcel Dekker: New York, 1991.

(16) Meyer, K.; Bendix, J.; Bill, E.; Weyhermüller, T.; Wieghardt, K. *Inorg. Chem.* Submitted.

term taking into account the anisotropy of the line width.[17] From this simulation an isotropic hyperfine coupling constant $A = 88 \times 10^{-4}$ cm^{-1} and an isotropic $g_{iso} = 2.001$ was calculated. The spectrum of a frozen solution at 10 K displays an axial signal with $g_{zz} = 2.003$, $g_{yy} = g_{xx} = 1.999$ and $A_{zz} = 187 \times 10^{-4}$ cm^{-1}, $A_{yy} = A_{xx} = 60 \times 10^{-4}$ cm^{-1}. Similar values have recently been reported by us for $[Mn^{VI}(N)(CN)_4]^{-}$ [18] and for a tetrahedral manganese(VI) species.[19] These spectra are in excellent agreement with the expected d^1 electronic configuration of a C_{4v}-symmetric Mn(VI) species.

Vibrational Spectrosocopy. Infrared and Raman ($\lambda = 1064$ nm) spectra of solid samples of complexes have been recorded as KBr disks; the results are summarized in Table S1.

It is well established that cis and trans isomers of coordinated cyclam are readily distinguished by their vibrational characteristics in region 800−900 cm^{-1} where the wagging and rocking deformation bands, γ(N−H) and $\delta(CH_2)$, of the amine and methylene groups, respectively, give rise to two vibrational modes for trans configurated complexes but four to five in the cis analogues.[20] Thus complexes **1**−**6** display these modes at 880 ± 10 cm^{-1} (γ(N−H)) and 810 ± 5 (δ(C−H)), whereas for **7** four bands at 866, 856, and 815, 806 are observed. These vibrational modes are, in general, not affected by differing counteranions and are therefore diagnostic.

Complexes containing a terminal azide ligand display an intense antisymmetric stretching frequency, $\nu_{as}(N_3)$, at ∼2070 cm^{-1}, and a symmetric $\nu_s(N_3)$ mode at ∼1350 cm^{-1} and a deformation band at ∼620 cm^{-1}. The first of these is readily detected in the infrared. For complexes **1** and **9** the $\nu_{as}(N_3)$ vibration is observed at 2069, 2046 cm^{-1} and 2063, 2032 cm^{-1}, respectively, and for $[LMn^{III}(N_3)_3]$ at 2067, 2027 cm^{-1}. In complexes containing a 1,3-bridging azide as in **2** and **8** the $\nu_{as}(N_3)$ frequency is shifted to higher energy at 2113 and 2111 cm^{-1}, respectively.

The ν(Mn≡^{14}N) stretching frequency in complexes **2**−**7** and **9** has been observed in the range 977 cm^{-1} in **9** to 1045 cm^{-1} in **5**. Obviously, this mode is quite sensitive to the presence (or absence) and the nature of the sixth ligand in trans position to this group. The coordinated acetonitrile in **4** is a very weakly bound ligand, and, consequently, the Mn≡N distance is short. In five-coordinate $[Mn(N)(CN)_4]^{2-}$ the ν(Mn≡^{14}N) mode has been observed at 1094 cm^{-1}.[18] In contrast, in **7** and **9** the sixth ligand is a relatively strong σ-donor amine nitrogen, and the ν(Mn≡^{14}N) is observed at 1005 and 977 cm^{-1}, respectively, which is similar to the previously reported value of 983 cm^{-1} for $[LMn^{V}(N)(acac)]PF_6$. In some cases (**2**, **4**, **6**, **7**) the assignment of the ν(Mn≡^{14}N) vibration has been corroborated by the spectra of the Mn≡^{15}N isotopomers which were synthesized from **1** by using ^{14}N−^{14}N−^{15}N labeled sodium azide (a 1:1 Mn≡^{14}N, Mn≡^{15}N isotopomer mixture is thus obtained). A shift of the ν(Mn≡^{15}N) mode to lower frequencies by 26−30 cm^{-1} is in excellent agreement with a two-mass harmonic oscillator model (calc. 27−29 cm^{-1}).

In the solid-state Raman spectrum of **4** the ν(C≡N) stretching mode of the coordinated CH_3CN ligand is observed at 2263 cm^{-1} which is only 4 cm^{-1} lower in energy than in uncoordinated acetonitrile. Clearly, this ligand is very weakly bound. Complex **7** displays a ν(CN) stretching frequency at 2122 cm^{-1} which may be compared with the values of 2126 and 2115 cm^{-1} reported for $[PPh_4]_2[Mn^{V}(N)(CN)_4]\cdot 2H_2O$.[18]

NMR Spectroscopy. Complexes **2**−**7** and **9** possess a low-spin d^2 electron configuration, and, consequently, ^{1}H and ^{13}C spectra of these compounds are observable. The chemical shifts of proton and carbon resonances are not affected by the substantial temperature-independent paramagnetism; they are observed in the normal regions with normal line widths as is expected for diamagnetic compounds. These results will be reported elsewhere.

We have also measured ^{15}N NMR spectra of samples where the terminal nitrido group was labeled with ^{15}N in d_3-acetonitrile solutions (**4**, **6**, and **7**). Chemical shifts are referenced versus d_3-nitromethane ($\delta(CH_3{}^{15}NO_2) \equiv 0$ ppm). Only, two resonances are observed: one at $\delta = -135.4$ ppm which is due to the solvent and a second signal at unprecedentedly low field at 692.9 ppm for **4**, 698.9 ppm for **6**, and at 693.9 ppm for **7** which is assigned to the corresponding Mn^{V}≡^{15}N group. The linewidth of these signals is small ($\nu_{1/2} < 1$ Hz). These chemical shifts of the Mn≡^{15}N unit exceed those reported for second- and third-row transition metal nitrides[21−23] (Table S2) and indicate an enormous deshielding of the nitrido nuclei in manganese(V) species.

By using ^{1}H−^{15}N inverse correlation NMR spectroscopy we have also been able to detect the ^{15}N signals of the amine nitrogens (natural abundance) of the coordinated cyclam ligand in **4**. As shown in Figure S2 two ^{15}N signals at −349 and −368 ppm are in excellent agreement with its C_s symmetric Mn(cyclam) fragment.

Magnetic Susceptibility Measurements. The molar magnetic susceptibilities of triply recrystallized solid samples of complexes **2**, **3**, **4**, **6**, **7**, and **9** have been measured in the temperature range 5−300 K by using a SQUID magnetometer in an external field of 1.0 T. The experimental data, χ_{obsd}, were corrected for underlying diamagnetism, χ_{DIA}, by using Pascal's tabulated constants[24] and for a small paramagnetic impurity (pi) with $S = 2$ which was calculated by a fitting procedure of the low-temperature data (2−50 K). In all cases the resulting values for the magnetic susceptibilities are positive and are within experimental error temperature-independent corresponding, therefore, to a significant temperature-independent paramagnetism (TIP) ($\chi_{TIP} = 110-120 \times 10^{-6}$ cm^3 mol^{-1}). Table S3 summarizes these results.

This TIP is composed of a component perpendicular and parallel to the Mn≡N axis, $\chi_{TIP}{}^{\parallel}$ and $\chi_{TIP}{}^{\perp}$, and results from mixing of the nonmagnetic ground state $^1A_1$ with the also nonmagnetic excited states by the spin−orbit operator **L**. The parallel component is exclusively generated by mixing of the $^1A_1$ ground state with the excited $^1A_2$ state, whereas the perpendicular component (98%) is due to the interaction with the energetically lowest lying excited ^{1}E state. By using the angular overlap model (AOM) parameters $e_\sigma{}^{ax} = 26\,800$ cm^{-1}, $e_\pi{}^{ax} = 18\,800$ cm^{-1}, $e_\sigma{}^{cyc} = 7300$ cm^{-1}, and a Racah parameter B of 400 cm^{-1} from the ligand field model described below

(17) Glerup, J.; Weihe, H. *Acta Chem. Scand.* **1991**, *45*, 444.
(18) Bendix, J.; Meyer, K.; Weyhermüller, T.; Bill, E.; Metzler-Nolte, N.; Wieghardt, K. *Inorg. Chem.* **1998**, *37*, 1767.
(19) (a) Danopoulos, A. A.; Wilkinson, G.; Sweet, T. K. N.; Hursthouse, M. B. *J. Chem. Soc., Dalton Trans.* **1994**, 1037. (b) Danopoulos, A. A.; Wilkinson, G.; Sweet, T. K. N.; Hursthouse, M. B. *J. Chem. Soc., Dalton Trans.* **1995**, 937.
(20) (a) Poon, C. K. *Inorg. Chim. Acta* **1970**, *5*, 322. (b) Baldwin, M. E. *J. Chem. Soc. (London)* **1960**, 4396. (c) Poon, C. K.; Pun, K. C. *Inorg. Chem.* **1980**, *19*, 568. (d) Chan, P. K.; Poon, C. K. *J. Chem. Soc., Dalton Trans.* **1976**, 858. (e) Chan, P. K.; Isabirye, D. A.; Poon, C. K. *Inorg. Chem.* **1975**, *14*, 2579.
(21) Dilworth, J. R.; Donovan-Mtunzi, S.; Kan, C. T.; Richards, R. L. *Inorg. Chim. Acta* **1981**, *53*, L161.
(22) Donovan-Mtunzi, S.; Richards, R. L.; Mason, J. *J. Chem. Soc., Dalton Trans.* **1984**, 1329.
(23) Laplaza, C. E.; Johnson, M. J. A.; Peters, J. C.; Odom, A. L.; Kim, E.; Cummins, C. C.; George, G. N.; Pickering, I. J. *J. Am. Chem. Soc.* **1996**, *118*, 8623.
(24) *Theory and Application of Molecular Diamagnetism*; Mulay, L. N., Boudreaux, E. A., Eds.; Wiley-Interscience: New York, 1976.

Table 1. Structural Parameters of $[(cyclam)Mn^{V}(N)Y]^{n+}$ Complexes

complex	Mn≡N, Å	Mn−N_{eq},[a] Å	Mn−Y, Å	θ,[b] deg	N≡Mn−Y, deg	d,[c] Å
1		2.043(3)	2.171(3)	90.0(3)		0
2	1.523(7)	2.015(8)	2.282(8)	97.0(3)	177.8(4)	0.246, 0.235
3	1.531(2)	2.035(2)	2.636(1)	96.6(1)	176.4(1)	0.236
4	1.518(5)	2.027(5)	2.409(5)	97.0(3)	176.9(2)	0.253
5	1.514(2)	2.028(3)	2.511(2)	98.5(1)	174.5(1)	0.299
6	1.530(4)	2.032(4)	2.214(3)	96.5(2)	178.7(2)	0.232, 0.242
7	1.539(2)	2.060(2)[d]	2.303(2)	96.2(1)[d]	172.4(1)	0.204
		1.997(2)[e]		91.7(1)[e]		

[a] Average of the four Mn−N_{amine} bonds of coordinated cyclam. [b] Average of the four N≡Mn−N_{amine} bond angles. [c] Distance of Mn ion above the best plane defined by four cyclam nitrogen atoms. [d] Average of three equatorial Mn−N_{amine} bonds and N≡Mn−N_{amine} bond angles. [e] Mn−C bond distance and N≡Mn−C bond angle.

one can calculate $\chi_{TIP} = 118 \times 10^{-6}$ cm^3 mol. This is not a fit to the data but represents a calculated value using spectroscopically determined ligand-field parameters. The agreement with the experimental values for χ_{TIP} is gratifying.

For the dinuclear complex **8** the magnetic moment, μ_{eff}, was found to decrease from 7.40 μ_B per dimer at 290 K to 1.33 μ_B at 5 K indicating antiferromagnetic coupling between two high-spin Mn^{II} ions ($S = {}^5/_2$) yielding a diamagnetic ground state. The temperature-dependence of the magnetic moment was successfully modeled by using the Heisenberg, Dirac, van Vleck model for intramolecular exchange coupling with the spin-Hamiltonian $H = -2JS_1 \cdot S_2$ ($S_1 = S_2 = {}^5/_2$) and $g = 2.0$ (fixed). A small amount of a mononuclear paramagnetic impurity with $S = 2$ of 3.3% was taken into account (fit parameter). A J value of -7.5 cm^{-1} gives a satisfactory fit which is typical for bis-μ(1,3-N_3) bridged manganese(II) ions and confirms therefore the proposed structure for **8**.[25]

Crystal Structures. The molecular structures of complexes **1**−**7** have been determined by X-ray crystallography. Table 1 summarizes some pertinent structural parameters of the first coordination sphere of the corresponding cation.

All cations in complexes **1**−**6** contain an equatorially coordinated cyclam ligand. Of the five possible stereoisomers, *trans*-III according to Bosnich et al.[26] is the energetically most favored (least strained) form which prevails in all complexes. Only the cation in **7** contains a *cis*-coordinated macrocyclic amine.

The Mn−N_{amine} distances in **1**−**6** are within experimental error equidistant at 2.03 ± 0.01 Å irrespective of the fact that in **1** a high spin d^4 Mn^{III} ion is present, whereas in **2**−**6** the oxidation state of the manganese ion is formally +V. In **7** the three equatorial Mn−N_{amine} distances are slightly longer at 2.060(2) Å but the axial Mn−N_{amine} in *trans*-position to the Mn≡N group is significantly longer at 2.303(2) Å due to a pronounced structural *trans*-influence of the nitrido group.

In the following we discuss some peculiarities of individual structures: In complex **1** containing a Jahn−Teller manganese(III) ion (d^4) the two coordinated azide ligands are in *trans*-position relative to each other (Figure 3); the average Mn−N_{azide} distance at 2.171(3) Å is longer than the corresponding equatorial Mn−N_{amine} distances. In the analogous complex *trans*-[(cyclam)$Cr^{III}(N_3)_2$](ClO_4) the average Cr−N_{amine} and Cr−N_{azide} distances are 2.062(4) Å and 1.977(4), respectively.[16] Thus the Cr−N_{azide} bonds are *shorter* than the Cr−N_{amine} bonds; the opposite is true in **1** indicating thereby that the N_3−Mn^{III}−N_3 unit represents the Jahn−Teller axis of an elongated octahedron. The two crystallographically independent cations in **1** are not quite identical although both possess crystallographically imposed C_i symmetry: the average Mn−N_{azide} bond distances in both cations are at 2.167(3) Å and 2.175(3) Å, respectively, where the difference is only barely significant within the 3σ limit, but the Mn−N_α−N_β bond angles at 136.9(4)° and 130.6(3)° differ significantly. This accounts for the observation of *two* $\nu_{as}(N_3)$ stretching frequencies of equal intensity in the infrared spectrum of **1**.

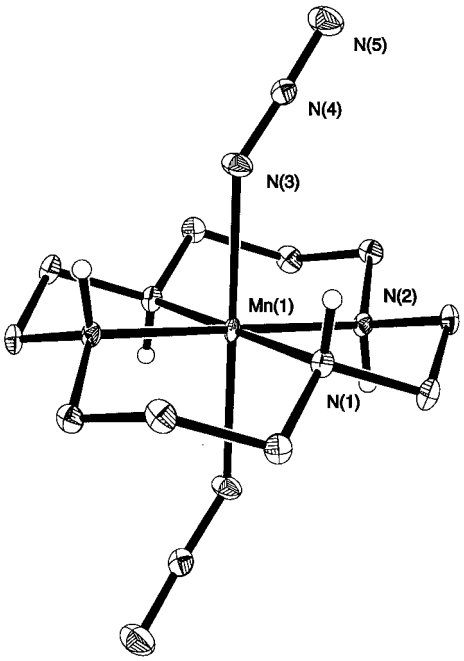

Figure 3. Perspective view of one of the two crystallographically independent *trans*-$[Mn^{III}(cyclam)(N_3)_2]^+$ cations in crystals of **1**.

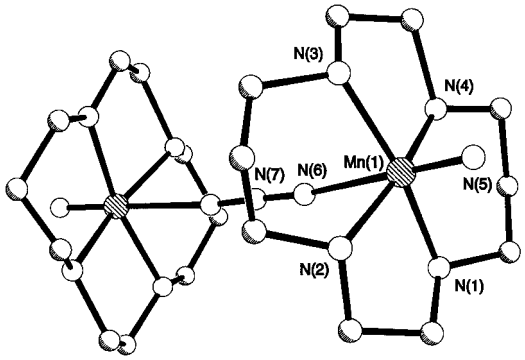

Figure 4. Perspective view of one of the two crystallographically independent dinuclear trications in crystals of **2**.

Complex **2** contains the μ-1,3-azido bridged dinuclear trication [{*trans*-[(cyclam)Mn^{V}(N)]}$_2$(μ-N_3)]$^{3+}$ (Figure 4). There are two crystallographically independent cations of very similar

(25) Escuer, A.; Vicente, R.; Goher, M. A. S.; Mautner, F. A. *Inorg. Chem.* **1996**, *35*, 6386.

(26) (a) Bosnich, B.; Poon, C. K.; Tobe, M. L. *Inorg. Chem.* **1965**, *4*, 1102. (b) Adam, K. R.; Atkinson, I. M.; Lindoy, L. F. *Inorg. Chem.* **1997**, *36*, 480.

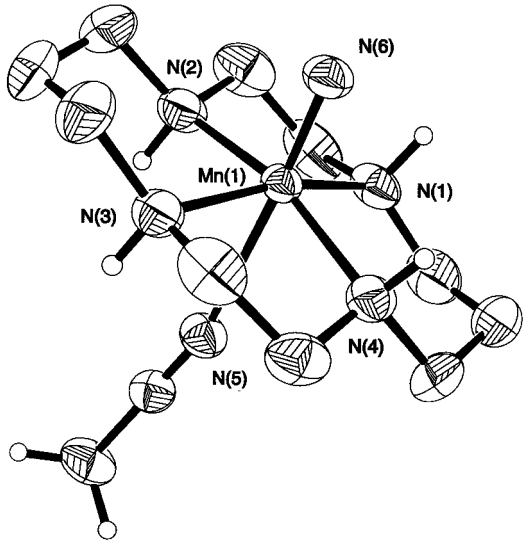

Figure 5. Perspective view of the dication *trans*-[Mn^{V}(cyclam)(N)-($NCCH_3$)]$^{2+}$ in crystals of **4**.

dimensions in the unit cell. The Mn≡N bond is short and exhibits considerable triple bond character. This is also true for complexes **3**−**6** containing the (N)Mn^{V}(cyclam)-fragment where the Mn−$N_{nitride}$ bond length varies slightly between 1.518-(5) Å in **4** and 1.531(2) Å in **3** as a function of the nature of the sixth ligand Y in *trans*-position. In **2** this sixth coordination site is occupied by a linearly bound 1,3-azido bridge: N≡Mn−N_{azide} 177.8(4)° and 176.6(4)°, respectively, and Mn−N_{α}−N_{β} 171.6(9)° and 172.9°. As a consequence, the two planes each defined by the four equatorial amine nitrogen atoms are tilted by 10.2°. In all complexes containing the *trans*-Mn(N)(cyclam)-fragment the manganese(V) ion is positioned above this plane of four amine nitrogen atoms by 0.20−0.30 Å. As a measure for this distortion the average bond angle N≡Mn−N_{cyclam}, θ, has been compiled in Table 1; at 90° the Mn(V) ion would be in the plane; experimentally this angle is found in the range 96.5−98.5°.

The Mn−N bond distance of 2.409(5) Å to the coordinated acetonitrile molecule in **4** (Figure 5) is quite long, and, therefore, this bond is weak contrasting in this respect the Mn−N_{azide} bond length at 2.282(8) Å in **2**. Complex **3** has a weakly bound chloro ligand in the sixth position (Figure S3).

In complexes **5** and **6** the monocations have a weakly coordinated ClO_4^- and a $CF_3CO_2^-$ anion bound at the sixth coordination site of the N≡Mn(cyclam)-fragment, respectively (Figure 6). The Mn−O(23) bond at 2.511(2) Å in **5** is very weak indeed. Interestingly, the monodentate ClO_4^- anion forms a weak intramolecular O···H−N hydrogen bonding contact to one amine hydrogen atom of the cyclam ligand. In the present series of nitridocyclammanganese(V) complexes the perchlorate anion represents the weakest ligand and, consequently, the Mn≡N bond is the shortest, the angle θ is the largest, and the out-of-plane shift of the Mn^{V} ion reaches a maximum at 0.299 Å. In **6** the $CF_3CO_2^-$ is also a weakly coordinated monodentate ligand (Mn(1)−O(1) 2.214(3) Å) where the uncoordinated carbonyl oxygen O(2) forms an inter- and an intramolecular O···H−N hydrogen bonding contact.

Crystals of **7** contain discrete *cis*-[(cyclam)Mn(N)(CN)]$^{+}$ monocations (Figure 7) and uncoordinated ClO_4^- anions. The macrocycle cyclam is coordinated in its *cis*-configuration to the Mn^{V} ion. A coordinated cyanide is in *cis*-position relative to the terminal nitrido ligand. Thus the manganese ion is in a distorted octahedral environment. The Mn≡N bond at 1.539-

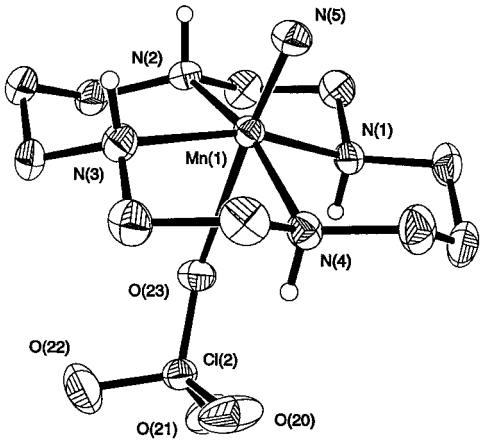

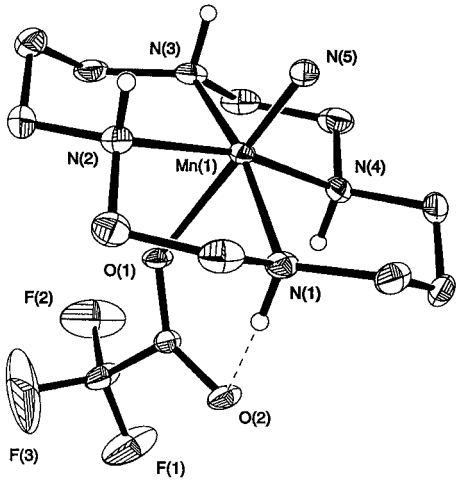

Figure 6. Perspective views of the monocations *trans*-[Mn^{V}(cyclam)-(N)(ClO_4)] (top) and *trans*-[Mn^{V}(cyclam)(N)(O_2CCF_3)]$^{+}$ (bottom) in crystals of **5** and **6**, respectively.

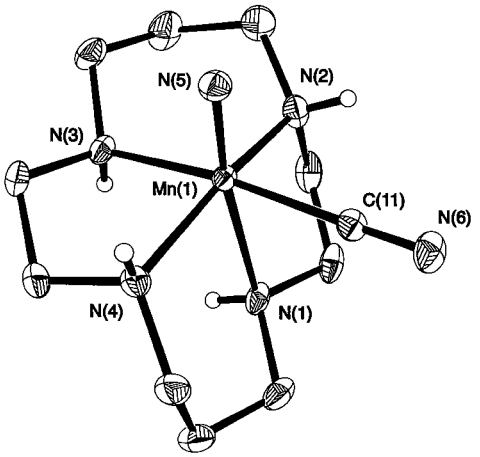

Figure 7. Perspective view of the monocation *cis*-[Mn^{V}(cyclam)(N)-(CN)]$^{+}$ in crystals of **7**.

(2) Å is the longest in the series of nitrido complexes, whereas the Mn−N_{amine} bond in *trans*-position is comparatively strong at 2.303(2) Å. Very similar behavior has been reported previously for [LMn^{V}(N)(acac)][BPh_4].[9]

Electronic Structures of Complexes. The electronic spectra of complexes **2**−**7** and **9** have been recorded in the range 250−

Table 2. Electronic Spectra of Complexes in Solution

		absorption maximum, nm (ϵ, M^{-1} cm^{-1})			
complex	solvent	I	II	III	IV
2	CH_3CN	810(4)	584(65)	492(51)	*a*
4	CH_3CN	850(1)	581(34)	496(24)	
	H_2O	844(1)	581(28)	495(19)	310(15)
	9.2 M $HClO_4$ ($NaClO_4$)	830(1)	570(27)	493(21)	329(12)
5	CH_3NO_2	820(1)	573(29)	497(23)	*a*
6	CH_3CN	850(1)	585(27)	~500'(sh)	~360(sh)
7	H_2O (0.1 M NaCN)	850(<1)	575(30)	498(30)	~350(sh)

[a] Band not observed due to overlap with azide-to-metal charge-transfer bands or solvent absorption (CH_3NO_2).

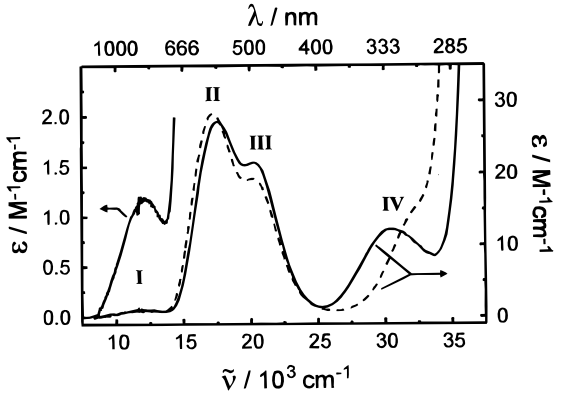

Figure 8. Electronic spectra of **4** recorded in H_2O (- - -) and 9.2 M $HClO_4$ (—).

1600 nm in a variety of solvents. The results are summarized in Table 2. A general problem of these solution spectra is associated with the fact that the sixth ligand in *trans*-position to the five-coordinate $[N{\equiv}Mn^{V}(cyclam)]^{2+}$ fragment is very weakly bound and, consequently, labile in solution. For instance, the spectra of **4** and **5** recorded in H_2O differ slightly from the spectra of the same complexes measured in 9.2 M $HClO_4$ which are identical with the spectra measured in concentrated aqueous $NaClO_4$ solution which in turn are identical with the spectrum of **5** recorded in CH_3NO_2 solution in the range 350−1000 nm. We conclude that in water the species *trans*-$[(cyclam)Mn(N)]^{2+}$ or the six-coordinate complex $[(cyclam)Mn(N)(H_2O)]^{2+}$ prevails, whereas in concentrated aqueous perchlorate solutions ($HClO_4$ *or* $NaClO_4$) $[(cyclam)Mn(N)(ClO_4)]^{+}$ is the dominant species as in CH_3NO_2 solutions of **5**. This is shown in Figure 8. Remarkably, the spectra of all complexes containing the *trans*-$[(cyclam)Mn^{V}(N)Y]^{n+}$ unit are very similar, indeed.

The spectra each display four d−d transitions of very low intensity: a weak band I in the range 800−1100 nm ($\epsilon \sim 1$ M^{-1} cm^{-1}), two bands, II and III, in the visible region 400−700 nm ($\epsilon < 30$ M^{-1} cm^{-1}), and a band IV at ~320 nm ($\epsilon \sim 12$ M^{-1} cm^{-1}). The latter is often observed as shoulder only due to intensive tailing of charge transfer bands <300 nm. These four absorption maxima are most clearly detected in the spectrum of **4** shown in Figure 8 (solid line).

Single-crystal polarized absorption spectra of **2** have been recorded at room temperature and at 15 K. Orthorhombic crystals of **2** are strongly dichroic; thin hexagonal plates viewed perpendicular to the apparantly hexagonal face [010] are deep-violet (to black). In contrast, they are nearly colorless when viewed down the crystal in a 90° tilted crystal with the electric field vector of the polarized light parallel to the *z*- or *b*-axis. The molecular axis *z* is defined by the N≡Mn−N−N−N−

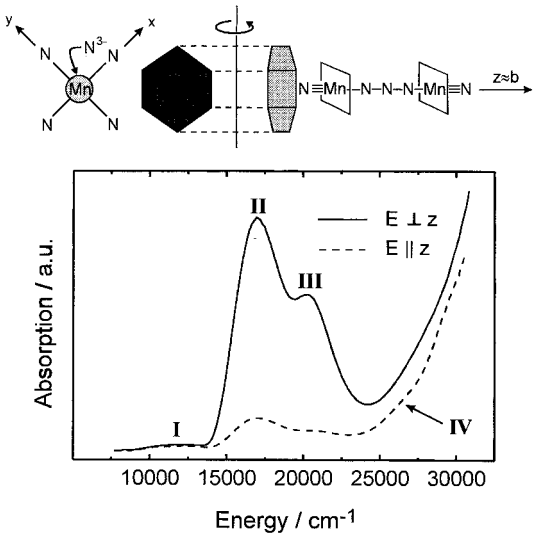

Figure 9. Polarized single-crystal electronic spectrum of **2** at 20 °C.

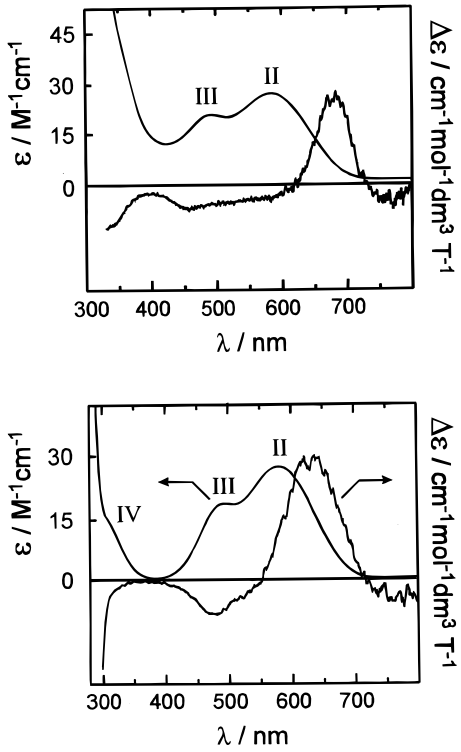

Figure 10. Magnetic circular dichroism spectra of **2** in CH_3CN (top) and **4** in H_2O (bottom) at 20 °C.

Mn≡N vector of the dinuclear cation in **2**, and this axis runs nearly parallel to the crystallographic *b*-axis. Due to the small deviation of the angle $Mn-N_{\alpha}-N_{\beta}$ of the bridging azide from exact linearity the Mn≡N *z*-vectors have a small inclination angle of ~4° relative to the crystallographic *b*-axis. As is shown in Figure 9 the electronic transitions II and III at 584 and 492 nm are strongly polarized in the molecular *xy*-plane, whereas transition I is not polarized. Transition IV at ~360 nm is only detectable as a shoulder in the E||z-spectrum (E||b); it also appears to be *xy*-polarized. Spectra recorded at 15 K are identical; the transitions I−IV are temperature-independent.

Figure 10 displays the magnetic circular dichroism (MCD) spectra of **4** in water where the $[(cyclam)Mn(N)(H_2O)]^{2+}$ species prevails and of **2** in acetonitrile at ambient temperature. These spectra clearly show that only band II corresponds to a transition into a degenerate orbital because only this transition possesses

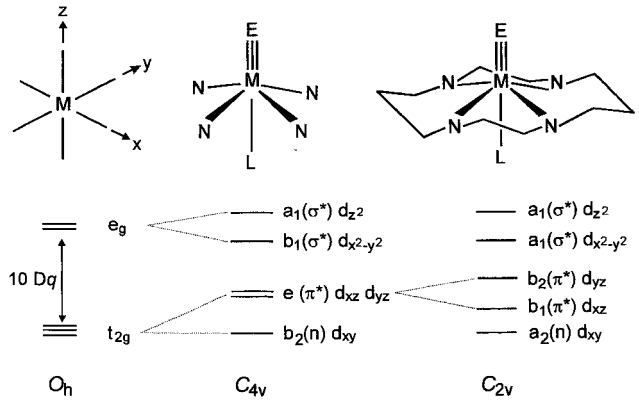

Figure 11. One-electron metal orbital schemes in octahedral and tetragonally distorted symmetry C_{4v} and C_{2v}.

A term character. Since the negative component of the first MCD band is at higher energy it is a negative A term. Band III gives rise to an overlapping B-term. Therefore, band II can safely be assigned to the spin and symmetry allowed transition $^1A_1 \rightarrow {}^1E$ (see below). Since the spin-paired d^2 ground state is nondegenerate the excited state must be degenerate.

In the following we attempt to assign the above spectra by adapting the scheme of terms originally introduced for vandyl, chromyl, and molybdenyl complexes by Gray and Ballhausen[27a] and which has also been used for *trans*-dioxo and nitrido complexes of Tc(V), Re(V), and Os(VI).[27,28] Figure 11 shows the conventions we will use. Strictly speaking, the $[N{\equiv}Mn^V$-(cyclam)$]^{n+}$ complexes possess C_{2v}- or C_s-symmetry due to the fact that two five- and two six-membered chelate rings are formed by the ligand cyclam yielding the trans III conformation, but it is sufficient to discuss the spectra by assuming C_{4v}-symmetry of the first coordination sphere surrounding the Mn^V ion.

In the ground state ($^1A_1$), the formally nonbonding $b_2(xy)$ level is filled, and the unoccupied $d\pi^*$ levels, e(xz,yz), are degenerate and have antibonding character. The higher-lying $b_1(x^2-y^2)$ and $a_1(z^2)$ orbitals are then σ-antibonding. Lowering the symmetry from C_{4v} to C_{2v} lifts the degeneracy of the $d\pi^*$ levels to $b_1(xz)$ and $b_2(yz)$.

The extremely weak band I in the visible at $\sim$12 000 cm^{-1} is assigned to the spin-forbidden transition $^1A_1 \rightarrow {}^3E$ which has not been observed previously for any nitridomanganese(V) species. This singlet $\rightarrow$ triplet transition has been reported for the d^2 systems *trans*-$[(L)_4Re(O)_2]^n$ (L = CN^-, $n = 3-$; $^1/_2$en, py; $n = 1+$)[27b,c] and for $[Os(N)Cl_4]^-$.[29]

Bands II, III, and IV have larger molar extinction coefficients and are typical for spin-allowed d−d transitions. The assignment of bands II and III of nearly equal intensity is not straightforward because the energy of the x^2-y^2 orbital relative to the degenerate $d\pi^*$ (xz,yz) level is strongly dependent on structural parameters, in particular, the Mn≡N bond strength. In a simple one-electron scheme this means that an increasing M≡N bond strength stabilizes the x^2-y^2 orbital (by increasing the angle θ, cf. Figure 13) and at the same time destabilizes

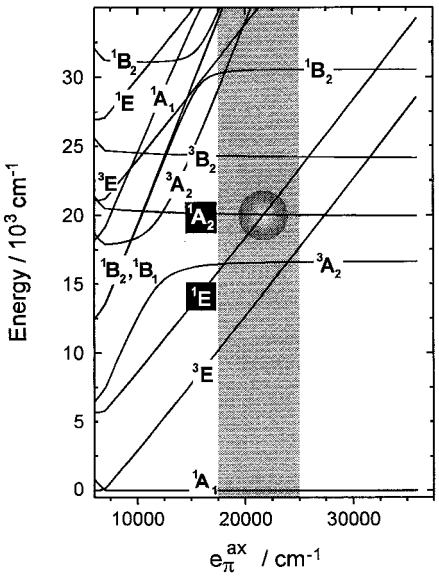

Figure 12. Calculated Tanabe−Sugano diagram for a $3d^2$ electron configuration in a C_{4v} symmetric ligand field as a function of the π-donor strength, e_π^{ax}, of the nitrido ligand ($e_\sigma^{ax} = 26\,800$ cm^{-1}; $e_\sigma^{cyclam} = 7300$ cm^{-1}; Racah $B = 400$ cm^{-1}). The shaded area is relevant for the present series of $[Mn(cyclam)(N)Y]^{n+}$ complexes. The shaded circle highlights the energy reversal of the degenerate (xz),(yz) orbitals and the (x^2-y^2) orbital, ref 30.

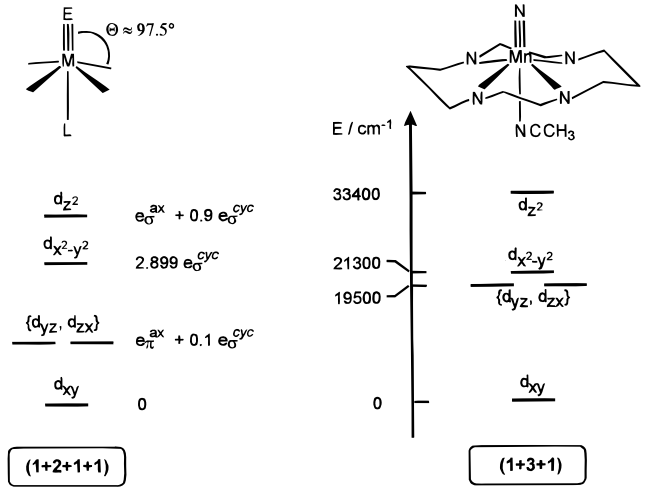

Figure 13. Orbital splitting diagram for axial systems with a single strong π-donor ligand (E = O^{2-}, N^{3-}) and calculated orbital energies for **4**.

the $d\pi^*$. Fujii et al.[30] have shown that in five-coordinate oxo- and nitridochromium(V) complexes this may lead to a reversal of the order of energy of the degenerate (xz), (yz), and the (x^2-y^2) orbitals. The lowest energy spin-allowed transition would thus be either $^1A_1 \rightarrow {}^1E$ (a) **or** $^1A_1 \rightarrow {}^1A_2$ (b).

For the present series of octahedral *trans*-$[(cyclam)Mn^V$-$(N)Y]^{n+}$ complexes the *out-of-plane* shift of Mn^V ion is rather small (0.24−0.30 Å) in contrast to the five-coordinate oxo- or nitridochromium(V) complexes considered by Fujii et al.[30] (0.42 Å), and, therefore, we expect case (a) to be valid. This is unambiguously proven by the MCD spectra where only band II displays a negative A term behavior. Thus we assign band II to a transition into the degenerate $d\pi^*$ level: $^1A_1 \rightarrow {}^1E$. Band III corresponds then to the $^1A_1 \rightarrow {}^1A_2$ ((xy) $\rightarrow$ (x^2-y^2)) transition and band IV must be assigned to $^1A_1 \rightarrow {}^1B_1$ ((xy) $\rightarrow$ (z^2)).

(27) (a) Ballhausen, C. J.; Gray, H. B. *Inorg. Chem.* **1962**, *1*, 111. (b) Winkler, J. R.; Gray, H. B. *J. Am. Chem. Soc.* **1983**, *105*, 1373. (c) Winkler, J. R.; Gray, H. B. *Inorg. Chem.* **1985**, *24*, 346.

(28) Miskowski, V. M.; Gray, H. B.; Hopkins, M. D. In *Advances in Transition Metal Coordination Chemistry*; Che, C.-M., Ed.; Yam, V. W. W., Co-Ed.; Jai Press Inc.: Greenwich, London, 1996; Vol. 1, pp 159−186.

(29) Cowman, C. D.; Trogler, W. C.; Mann, K. R.; Poon, C. K.; Gray, H. B. *Inorg. Chem.* **1976**, *15*, 1747.

(30) Fujii, H.; Yoshimura, T.; Kamada, H. *Inorg. Chem.* **1997**, *36*, 1122.

From group theoretical considerations, the transition II $^1A_1 \rightarrow {}^1E$ ($(xy) \rightarrow (xz,yz)$) is allowed and polarized perpendicular to the molecular *z* axis (*x*,*y*-polarized). This is in agreement with the polarized single crystal spectra: band II is the most intense absorption and it is *x*,*y*-polarized. On the other hand, band III is also strongly *x*,*y*-polarized. The strict group theoretical selection rules are not valid if coupling of the electronic dipole transitions with suitable vibrations (vibronic coupling) occurs. Alternatively, intensity stealing from an orbitally allowed CT band is also a viable mechanism. For vibronically allowed bands a temperature-dependence of their intensities is expected. This decrease of the intensity with decreasing temperature can be very small and escape experimental detection.[31] Thus intensity and polarization of band III is explained by coupling to vibrations of E-symmetry (ν(Mn−L_{eq})). The same mechanism has been invoked for the spectrum of $[VO(H_2O)_5]^{2+}$ where the transition $(xy) \rightarrow (x^2-y^2)$ has similar intensity and polarization as the $(xy) \rightarrow (yz)(xz)$ transition.[31]

The Angular-Overlap Model. We have calculated molecular orbital energy levels for the $[(cyclam)Mn^V(N)Y]^{n+}$ species as a function of the π-donor strength of the nitrido ligand by using the angular-overlap model (AOM). To do this the following reasonable assumptions were made: (a) the cyclam ligand is a pure σ-donor with one AOM parameter e_σ^{cyclam}; (b) the N≡Mn−Y bond angle is exactly 180° and this axis defines the molecular *z*-axis. The AOM parameters of the nitrido and its *trans*-ligand Y are described by one set of parameters e_σ^{ax} for σ-bonding and e_π^{ax} for π-bonding. Since the ligand Y is very weakly bound the above parameters essentially describe the Mn≡N bonding situation; (c) for the d^2 systems under consideration the Racah parameter $C = 4B$.

For the parameters e_σ^{ax}, e_π^{ax}, e_σ^{cyclam}, and *B* some plausible minimal and maximal values were established: e_σ^{cyclam} is ∼7000 cm^{-1} in *trans*-$[Cr^{III}(cyclam)(N_3)_2]ClO_4$ and *trans*-$[Cr^{IV}(cyclam)Cl_2]ClO_4$.[26] This value represents a lower limit since with increasing formal oxidation state of the metal ion e_σ^{cyclam} is expected to increase somewhat. The dependence of e_σ^{cyclam} on the oxidation state of the central metal ion can be judged from the series $[MoCl_6]^{3-/2-/1-}$ for which Δ_{Oh} values are 19 200, 22 000, and 24 100 cm^{-1}, respectively.[32] Thus, 10 000 cm^{-1} represents an upper limit for e_σ^{cyclam} in $Mn^V(N)(cyclam)$ complexes. The AOM parameters e_σ^{ax} and e_π^{ax} for the nitrido ligand were estimated by comparison with values reported by Gray et al.[29] for $[Os(N)Cl_4]^-$ where $\Delta(e-b_2) = e_\pi^{ax} = 36\,000$ cm^{-1} and $\Delta(a_1-b_2) = e_\sigma^{ax} = 49\,000$ cm^{-1}. Since the ligand-field splitting energy for transition metal ions of the second and third row are approximately twice as large as that of a first-row transition metal ion, we calculate e_π^{ax} as ∼18 000 cm^{-1} and e_σ^{ax} ∼24 500 cm^{-1} as lower limits for the Mn^V complexes.[33] Values for the spin−orbit coupling constant ζ_{3d} and the interelectronic repulsion parameters *B* and *C* for the free Mn^{5+} ion are 466, 1200, and 5100 cm^{-1}, respectively.[33] In a coordination compound these values are smaller due to the nephelauxetic effect of the ligands.

Figure 12 shows the calculated energy of states as a function of an increasing π-donor strength, e_π^{ax}, where the values for e_σ^{ax}, e_σ^{cyclam}, and *B* were held constant at 26 800, 7300, and 400 cm^{-1}, respectively. In the expected range of 18 000 to 25 000 cm^{-1} for e_π^{ax} (shaded area in Figure 12) the ^3E state is the energetically lowest first excited state which corresponds to the spin-forbidden $(xy) \rightarrow (xz,yz)$ transition (band I). With increasing energy at constant e_π^{ax} at 20 000 cm^{-1} the next excited state is $^3A_2$ which then corresponds to an also spin-forbidden transition $(xy) \rightarrow (x^2-y^2)$ followed by spin-allowed transitions to ^1E (band II) and $^1A_2$ (band III); the next spin-allowed transition is to $^1B_2$ (band IV). Interestingly, at values of e_π^{ax} larger than ∼25 000 cm^{-1} (shaded circle in Figure 12) the energy of $^1A_2$ is lower than that of ^1E.

The above AOM parameters reproduce the observed electronic spectrum of **4** and the susceptibility data (χ_{TIP}) well. As shown in Figure 13 an orbital splitting scheme (1+3+1) is relevant for the present complexes containing an $[Mn^V(cyclam)(N)]^{2+}$ fragment, whereas for vanadyl complexes a scheme (1+2+1+1) is more appropriate. This result is in excellent agreement with chemical intuition which predicts an M≡N group to be more covalent, i.e., the (*xz*),(*yz*) orbitals are more strongly destabilized and the (x^2-y^2) orbital is stabilized to a greater degree than in the corresponding oxometalates.

Finally, we have checked in which way a lower than C_{4v} symmetry (namely C_{2v}) of the $[(N)Mn^V(cyclam)]^{2+}$ fragment affects the degeneracy of the dπ* (*xz*,*yz*) orbitals (^3E). From the crystal structure determinations it is clear that the N_{amine}−Mn−N_{amine} bond angles deviate by ±6° from 90° due to the alternating bite angles. The AOM expressions for the resulting orbital energies $b_1(xz)$ and $b_2(yz)$ are then $e_\pi^{ax} + 0.09\ e_\sigma^{cyclam}$ and $e_\pi^{ax} + 0.11\ e_\sigma^{cyclam}$, respectively. Thus the splitting is proportional to the σ-donating strength of the ligand cyclam. Using $e_\sigma^{cyclam} = 7300$ cm^{-1} one can easily calculate that lowering the symmetry from C_{4v} to C_{2v} lifts the degeneracy of dπ* level by maximally 200 cm^{-1}. Therefore, bands II and III ($\Delta E = 3000$ cm^{-1}) cannot result from a splitting of the E state in C_{4v} into B_1 and B_2 states in C_{2v} symmetry.

Experimental Section

Syntheses. The macrocycles 1,4,8,11-tetraazacyclotetradecane (cyclam) and 1,4,7-trimethyl-1,4,7-triazacyclononane were prepared according to published procedures.[34,35] $MnCl_2$ and aqueous NaOCl solution were purchased from Fluka; LiCl, NaN_3, and $AgClO_4$ and $(CF_3CO)_2O$ were obtained from Merck and Aldrich, respectively. Na($^{15}N^{14}N^{14}N$) (98%) was obtained from the Cambridge Isotope Laboratories. All solvents used were of analytical grade. Water-free CH_3CN used for the electrochemical experiments was freshly distilled from CaH_2 and stored over Al_2O_3. The precursor complexes *trans*-$[(cyclam)Mn^{III}Cl_2]Cl\cdot 5H_2O$[12] and $[LMn^{III}Cl_3]$[36] were synthesized as described in the literature.

Caution. Although we have not encountered any problems, it should be kept in mind that perchlorate salts, metal azides (dry AgN_3!), and HN_3 are potentially explosive and should be handled only in small quantities and with appropriate precaution.

***trans*-[(cyclam)$Mn^{III}(N_3)_2$]ClO_4 (1).** Green *trans*-$[(cyclam)MnCl_2]Cl\cdot 5H_2O$ (0.70 g; 1.55 mmol) was added to a solution of NaN_3 (2.0 g; 30.8 mmol) in a methanol/water mixture (9:1 vol; 50 mL) whereupon the color changed to orange-brown. The solution was stirred at 40−50 °C for 30 min and filtered. Careful addition of 1.0 M aqueous $HClO_4$ (caution: HN_3 evolution) to this solution and storage at 4 °C for 12 h produced a microcrystalline, orange precipitate of **1**. Recrystallization of this material from methanol/water (9:1) afforded octahedral single crystals suitable for X-ray crystallography. Yield: 0.50 g (75%). IR (KBr), cm^{-1}: $\nu(N_3)$ 2069, 2047. Anal. Calcd for $C_{10}H_{24}N_{10}$-

(31) Ballhausen, C. J.; Djurinskij, B. F.; Watson, K. J. *J. Am. Chem. Soc.* **1968**, *90*, 3305.

(32) (a) Runciman, W. A.; Schroeder, K. A. *Proc. Royal Soc. (London)* **1962**, *A265*, 489. (b) Horner, S. M.; Tyree, S. Y. *Inorg. Chem.* **1963**, *2*, 568.

(33) For the gaseous Mn^{5+} ion Racah B is 1200 cm^{-1} which is expected to be 40−80% of this value in coordination compounds: (a) Brorson, M.; Schäffer, C. E. *Inorg. Chem.* **1988**, *27*, 2522. (b) Jørgensen, C. K. *Oxidation Numbers and Oxidation States*; Springer-Verlag: Berlin, 1969.

(34) Barefield, K. E.; Wagner, F. *Inorg. Synth.* **1976**, *16*, 220.

(35) Wieghardt, K.; Chaudhuri, P.; Nuber, B.; Weiss, J. *Inorg. Chem.* **1982**, *21*, 3086.

(36) Wieghardt, K.; Bossek, U.; Nuber, B.; Weiss, J.; Bonvoisin, J.; Corbella, M.; Vitols, S. E.; Girerd, J.-J. *J. Am. Chem. Soc.* **1988**, *110*, 7398.

Table 3. Crystallographic Data for **1**−**7**

	1	**2**	**3**	**4**	**5**	**6**	**7**
chem formula	$C_{10}H_{24}ClMnN_{10}O_4$	$C_{20}H_{54}Cl_3Mn_2N_{13}O_{15}$	$C_{10}H_{24}Cl_2MnN_5O_4$	$C_{12}H_{27}Cl_2MnN_6O_8$	$C_{10}H_{24}Cl_2MnN_5O_8$	$C_{12}H_{24}ClF_3MnN_5O_6$	$C_{11}H_{24}ClMnN_6O_4$
fw	438.78	932.99	404.18	509.24	468.18	481.75	394.75
space group	$P\bar{1}$	*Pnma*	*Pbca*	$P2_1/c$	$P2_1/c$	$P2_1/c$	$P2_1/c$
a, Å	9.462(1)	16.752(3)	13.101(2)	8.119(1)	9.378(2)	14.334(3)	6.592(1)
b, Å	9.511(1)	25.009(5)	10.896(2)	16.920(2)	13.134(3)	15.237(3)	13.638(2)
c, Å	11.434(1)	18.764(3)	23.203(4)	16.242(2)	15.158(3)	17.745(4)	19.010(3)
α, deg	79.45(2)	90	90	90	90	90	90
β, deg	81.07(2)	90	90	103.81(2)	99.88(3)	90.69(3)	93.99(2)
γ, deg	63.50(2)	90	90	90	90	90	90
V, Å	902.1(3)	7861(3)	3312.2(10)	2166.7(6)	1839.3(7)	3875.4(14)	1704.9(4)
Z	2	8	8	4	4	8	4
T, K	100(2)	173(2)	100(2)	293(2)	293(2)	100(2)	100(2)
ρ calcd, g cm^{-3}	1.615	1.577	1.621	1.561	1.691	1.651	1.538
diffractometer used	Siemens SMART	Siemens SMART	Siemens SMART	Siemens SMART	Enraf-Nonius CAD4	Enraf-Nonius CAD4	Siemens SMART
no. of data	4151	45187	30947	9583	3869	9140	16807
no. of unique data	3014	5121	4793	3613	3724	8852	4759
no. of params	239	479	295	260	235	543	236
μ(Mo Kα), cm^{-1}	9.21	9.24	11.43	9.06	10.58	8.87	9.59
R1[a]	0.0434	0.0941	0.0272	0.0731	0.0345	0.0733	0.0400
wR2[b] (all data)	0.1206	0.2257	0.0670	0.2324	0.0994	0.1985	0.0961

[a] Observation criterion: $I > 2\sigma(I)$. $R1 = \sum||F_o| - |F_c||/\sum|F_o|$. [b] $wR2 = [\sum[w(F_o^2 - F_c^2)^2]/\sum[w(F_o^2)^2]^{1/2}$ where $w = 1/\sigma^2(F_o^2) + (aP)^2 + bP$, $P = (F_o^2 + 2F_c^2)/3$.

$MnClO_4$: C, 27.37; H, 5.51; N, 31.92. Found: C, 27.69; H, 5.30; N, 31.66. This preparation represents a slight modification of the procedure reported by Chan and Poon.[12]

[{*trans*-[(cyclam)Mn(N)]}$_2$(*μ*-N$_3$)](ClO$_4$)$_3$·3H$_2$O (2). Photolysis of a suspension of **1** (0.60 g; 1.37 mmol) in methanol (100 mL) at −35 °C with 350 nm light in a Rayonet reactor for 6 h produced a clear deep blue solution from which upon addition of $NaClO_4 \cdot H_2O$ (3.0 g) a microcrystalline blue precipitate formed at −18 °C. During photolysis a constant stream of dry argon was passed through the solution. Recrystallization from an ethanol/methanol mixture (1:1) produced deep blue hexagonal prisms which were suitable for X-ray crystallography. Yield: 0.325 g (50%). IR (KBr), cm^{-1}: $\nu(N_3)$ 2114, 2036; ν(Mn≡N) 1031. Anal. Calcd for $C_{20}H_{54}N_{13}Mn_2Cl_3O_{15}$: C, 25.75; H, 5.83; N, 19.52. Found: C, 26.01; H, 5.74; N, 19.58.

***trans*-[(cyclam)Mn(N)Cl](ClO$_4$) (3).** To a suspension of *trans*-[(cyclam)$Mn^{III}Cl_2$]Cl·5H$_2$O (0.50 g; 1.1 mmol) in water (20 mL) was added dropwise an aqueous ammonia solution (25%). To this green-brown solution was added with stirring an aqueous NaOCl solution (2.0 mL; 13% active chlorine). After 15 min of stirring the solution was filtered and the precipitated MnO_2 was discarded. To the clear blue-violet solution was added $NaPF_6$ (1.0 g). Within a few days in an open vessel at ambient temperature microcrystalline blue platelets of *trans*-[(cyclam)Mn(N)Cl]PF_6 precipitated. Recrystallization from aqueous HCl (pH = 6) and addition of $NaClO_4 \cdot H_2O$ produced hexagonal crystals of **3** suitable for X-ray crystallography. Yield: 0.09 g (18%). Anal. Calcd for $C_{10}H_{24}N_5MnCl_2O_4$: C, 29.72; H, 5.98; N, 17.33. Found: C, 30.12; H, 5.84; N, 17.55.

***trans*-[(cyclam)Mn(N)(NCCH$_3$)](ClO$_4$)$_2$ (4).** To a suspension of **2** (0.50 g; 0.53 mmol) in CH_3CN (10 mL) was added $AgClO_4$ (0.11 g; 0.53 mmol). Careful warming with stirring of this solution produced of precipitate of AgN_3 which was filtered off. (**Caution:** AgN_3, when dry, is explosive. The wet precipitate was immediately dissolved in aqueous NH_3). To the clear blue-violet filtrate was added dry ethanol (10 mL). Upon storage of this solution at 4 °C for 12 h microcrystals of **4** formed which were recrystallized from an acetonitrile/toluene (1:1) mixture. The crystals obtained were of X-ray quality. Yield: 0.49 g (90%). Anal. Calcd for $C_{12}H_{27}N_6MnCl_2O_8$: C, 28.30; H, 5.34; N, 16.50. Found: C, 28.31; H, 5.35; N, 16.66.

***trans*-[(cyclam)Mn(N)(ClO$_4$)](ClO$_4$) (5).** A solution of **4** (0.51 g; 1.0 mmol) in freshly distilled, dry nitromethane (20 mL) was gently heated to 90−95 °C with stirring under an argon blanketing atmosphere until one-half of the solvent had evaporated. To the cooled and filtered solution dry toluene (10 mL) was added. Further slow reduction of the reaction volume by evaporation by passing a stream of argon gas through the solution produced blue single crystals of **5**. Yield: 0.43 g (90%). Anal. Calcd for $C_{10}H_{24}N_5MnCl_2O_8$: C, 25.66; H, 5.17; N, 14.96. Found: C, 25.58; H, 5.17; N, 15.02.

***trans*-[(cyclam)Mn(N)(OCOCF$_3$)](ClO$_4$) (6).** To a solution of **4** (0.51 g; 1.0 mmol) in CH_3CN (20 mL) was added trifluoroacetic anhydride (1.0 mL). The solution was carefully hydrolyzed by addition of water containing ethanol (∼96%). Upon reduction of the reaction volume by evaporation blue single crystals of **6** were obtained. Yield: 0.43 g (90%). Anal. Calcd for $C_{12}H_{24}N_5MnF_3ClO_6$: C, 29.85; H, 5.05; N, 14.52. Found: C, 29.91; H, 5.02; N, 14.54.

***cis*-[(cyclam)Mn(N)(CN)](ClO$_4$) (7).** Solid $AgClO_4$ (0.11 g; 0.53 mmol) was added with gentle warming and stirring to a solution of **2** (0.50 g; 0.53 mmol) in CH_3OH (25 mL). (**Caution:** AgN_3 is explosive when dry.) To the filtered blue-violet solution was added in small amounts NaCN (0.105 g; 2.12 mmol) The solution was heated to 40−45 °C for 20 min. Upon cooling a blue-violet precipitate formed which was recrystallized from a saturated aqueous solution. Single crystals of X-ray quality were obtained. Yield: 0.13 g (31%). Anal. Calcd for $C_{11}H_{24}N_6MnClO_4$: C, 33.47; H, 6.12; N, 21.29. Found: C, 33.25; H, 6.41; N, 21.43. IR(KBr), cm^{-1}: ν(CN) 2122; ν(Mn≡N) 1005.

[{LMn^{II}(N$_3$)}$_2$(*μ*-N$_3$)$_2$] (8). A solution of [$LMn^{III}(N_3)_3$] (0.42 g; 1.2 mmol) in dry CH_3CN (60 mL) was photolyzed at ambient temperature in a Rayonet reactor (253.7 nm) or, alternatively, with a mercury immersion lamp in an all quartz apparatus. Throughout this experiment a constant stream of argon gas was passed through the solution. The color of the solution changed from deep brown to colorless within 30−45 min, and a colorless precipitate of **8** formed. Yield: 0.36 g (97%). IR (KBr), cm^{-1}: $\nu(N_3)$ 2111, 2075, 2044. Anal. Calcd for $C_{18}H_{42}N_{18}Mn_2$: C, 34.84; H, 6.82; N, 40.63. Found: C, 34.87; H, 6.82; N, 40.58.

[LMn(N)(N$_3$)$_2$]·0.5toluene (9). A solution of [$LMn^{III}(N_3)_3$] (0.42 g; 1.2 mmol) in dry CH_3CN (60 mL) was photolyzed at −35 °C in a Rayonet reactor (350 nm). Through the solution was passed a constant stream of argon gas. Within 2 h the color of the brown solution changed to intensive blue. To the filtered solution was added an equal volume of toluene. Slow evaporation of the solvents at ambient temperature produced blue, needle-shaped microcrystalline **9** within a few days. This material is stable at 4 °C under an argon blanketing atmosphere but decomposes in air. Yield: 0.31 g (70%). IR (KBr), cm^{-1}: $\nu(N_3)$ 2063, 2032; ν(Mn≡N) 977. Anal. Calcd for $C_{12.5}H_{25}N_{10}Mn$: C, 40.54; H, 6.80; N, 37.82. Found: C, 39.9; H, 6.76; N, 38.02.

Physical Measurements. Infrared spectra (400−4000 cm^{-1}) and Raman spectra (100−3600 cm^{-1}) of solid samples were recorded on a

Perkin-Elmer 2000 FT-IR-/FT-NIR Raman spectrometer as KBr disk and powder samples, respectively. For the Raman spectra, a diode pumped Nd: YAG Laser (λ = 1064 nm) was used. Cyclic voltammetric and coulometric measurements were performed on EG & G equipment (potentiostat/galvanostat model 273A). Temperature-dependent magnetic susceptibilities of powdered samples were measured by using a SQUID magnetometer (Quantum Design) at 1.0 T (2.0−300 K). Corrections for underlying diamagnetism were made by using tabulated Pascal constants. X-band EPR spectra of frozen solutions were recorded on a Bruker ESP 200E spectrometer equipped with a helium flow cryostat (Oxford Instruments ESR 910). UV−vis−NIR spectra of solutions were recorded on a Perkin-Elmer Lambda 19 spectrophotometer in the range 200−1600 nm. Single-crystal absorption spectra were measured on a Cary 5E spectrometer fitted with a closed cycle helium refrigerator (Air products) for sample cooling to 15 K. Photolyses were performed in a Rayonet photochemical chamber reactor RPR-100 equipped with different lamp sets with emission maxima between 184.9 and 419 nm. NMR spectra were recorded on Bruker DRX 400 and DRX 500 instruments at 50.7 MHz (^{15}N) at room temperature. ^{15}N NMR spectra were referenced externally to the absolute frequency of 50.6969910 MHz which was the resonance frequency of neat nitromethane under the same experimental conditions ($\delta^{15}N(CH_3NO_2) \equiv 0$ ppm). ^{15}N NMR spectra were recorded in 5 mm tubes with a triple resonance indirect detection ^{1}H/^{15}N broad band (BB) probe. Rather than using the dedicated ^{15}N coil, the BB coil was used for ^{15}N detection to reduce interference with the lock signal (90° pulse: 16 μs at full power). Samples were 50% ^{15}N labeled at the terminal nitrido group and about 20 mg in 0.5 mL sample volume. Using 30° pulses, a ^{15}N signal was generally detected after about 300 scans. The signal from acetonitrile (δ = −136 ppm) solvent was generally much stronger in intensity than the signal of the sample and was used to check the scale of the spectrum and to verify that the nitrido signal was not folded.

X-ray Crystallographic Data Collection and Refinement of the Structures. Blue single crystals of **2**, **3**, **4**, and **6**, an orange crystal of **1**, and violet crystals of **5**, and **7** were mounted in sealed glass capillaries. Graphite monochromated Mo Kα radiation (λ = 0.71073 Å) was used throughout. Crystallographic data of the compounds are listed in Table 3. Intensity data for **5** and **6** were collected on an Enraf-Nonius CAD4 diffractometer using the ω-2θ scan technique. Data were corrected for Lorentz and polarization effects, but no absorption correction was carried out due to small absorption coefficients. Compounds **1**, **2**, **3**, **4**, and **7** were measured on a Siemens SMART CCD-detector system equipped with a cryogenic nitrogen cold stream. Cell constants were obtained from a subset of at least 3128 stronger reflections. Data collection was performed by a hemisphere run taking frames at 0.30° in ω. Corrections for Lorentz and polarization effects and a semiempirical absorption correction using the program SADABS[37] were applied. The Siemens ShelXTL[38] software package was used for solution, refinement, and artwork of the structures. All structures were solved and refined by direct methods and difference Fourier techniques performed on DEC Alpha workstations. Neutral atom scattering factors were obtained from tables.[39] All non-hydrogen atoms were refined anisotropically except those of disordered parts of the macrocycle and some perchlorate anions which were isotropically refined by split atom models. All hydrogen atoms were placed at calculated positions and refined as riding atoms with isotropic displacement parameters. Carbon and nitrogen atoms of the cyclam ligand in **2** were found to have large anisotropic thermal components along the C−C and C−N bonds in the macrocycle. This is due to a crystallographically imposed mirror plane bisecting the cation which in fact has a slightly lower symmetry. A split atom model was applied for some carbon atoms. Details are given in the Supporting Information.

Acknowledgment. We thank the Danish Research Council for granting the spectropolarimeter and Karen Jørgensen (University of Copenhagen) for measuring the MCD spectra. We are grateful to the University of Copenhagen (Chemistry Department) for granting leave of absence to J.B. We thank Dr. T. Brunold and Professor H. U. Güdel (University of Bern) for measuring the polarized single crystal electronic spectra. Financial support of this work from the Fonds der Chemischen Industrie is also gratefully acknowledged.

Supporting Information Available: Tables of crystallographic and structure refinement data, atom coordinates and U_{eq} values, bond lengths and angles, anisotropic thermal parameters, and calculated and refined positional parameters of hydrogen atoms for complexes **1**−**7** noncrystallographic information in Table S1 containing Mn≡N vibrations of complexes; Table S2 containing ^{15}N NMR data of complexes; Table S3 with magnetic susceptibility data of complexes; Schemes S1 and S2 displaying synthetic routes to complexes; Figure S1 displaying the cyclic and square-wave voltammogram of **4**; Figure S2 shows the ^{1}H−^{15}N inverse correlated NMR spectrum of **4**; and Figure S3 shows the structure of **3** (51 pages, print/PDF). See any current masthead page for ordering information and Web access instructions.

JA980686J

(37) Sheldrick, G. University of Göttingen: 1994.
(38) ShelXTL V.5; Siemens Analytical X-ray Instruments, Inc.: 1994.
(39) *International Tables for X-ray Crystallography*; Kynoch Press: Birmingham, U.K. 1991.